Chapter 1 Introduction

1.1 Preface

The unique and fascinating properties of nanostructured materials have triggered tremendous motivation among scientists to explore the possibilities of using them in industrial applications. In particular, the electronic and optical properties of nanostructured materials have been of interest for their potential applications in the fabrication of microelectronic and electroptical devices.[1-4] There are lots of advantages in reducing the size of microelectronics: higher density of integration, faster response, lower cost, and less power consumption. With the development of microelectronics and electroptical devices, the techniques for the fabrication of nanomaterials have been extensively study. Worldwide attention is focused on nanostructured materials of different shapes, as films, wires, and dots, for their different geometry of the nanoscale materials with many peculiar physical phenomena include size dependent excitation, ballistic conductance, Coulomb blockade, single electron tunneling and metal-insulator transition. These studies mainly focused on zero-dimensional (0D) quantum dots and two-dimensional (2D) quantum well structures, while study of one-dimensional (1D) nanowires could have distinctive opportunities in understanding fundamental concepts and can exhibit unusual physical properties, such as field emission,[5,6] electrical conductivity,[7-11] biological,[12] magnetism,[13] mechanical properties[14,15] and visible photoluminescence[16,17] due to quantum confinement effect,[18] which differ from the bulk materials. There are many nanoscale devices, such as quantum dot lasers,[19,20] single electron transistor (SET),[21] logic and memory units[22] and light-emitting diode (LEDs),[23] have been fabricated by numerous research group around the world.

1.2 Development and Research of Nanowires

Nanostructures can be defined as systems in which at least one dimension is smaller than 100 nm; that is reducing 1, 2, or 3 dimensions (D) of a bulk material to the nanoscale produces 2D films, 1D nanowires, or 0D nanoclusters, respectively. In the past few years, 1D nanostructured materials, such as nanowires,[24-26] nanorods,[27] nanotubes,[28] nanobelts[29,30] and nanocables,[31-34] have draw much attention in basic scientific research and technology applications. Nanowires are anisotropic nanoparticles with high aspect ratios (length/diameter). In general, they have diameters of 1-100 nm and length of several micrometers. Many singular characteristics have been reported including fundamentals of mesoscopic phenomenon[35] and the potential in the buildup of functional electronic, superior mechanic toughness, higher luminescence efficiency and lowered laser threshold and molecular computing to scanning probe microscopy tips. In addition, the nanowires can provide a material system to experimentally test fundamental quantum mechanical concepts.

1.2.1 Optical Properties

Due to the quantum confinement effect, the nanowires exhibit distinct optical properties[36,37] when their size is below certain critical dimension; the blue shift of absorption edge of nanowires from the bulk materials, sharp discrete absorbance feature and relatively strong photoluminescence were observed.[38] The quantum size confinement effect is a basic characteristic of all low dimensional materials. The electrical and optical properties of nanowires are strongly size dependent. It is widely accepted that the quantum confinement of electrons by the various potential well of

nanostructure control the electrical, optical, magnetic, and thermoelectric properties of the solid material. According to the solid state physics,[39] the dynamics of the electrons in crystals can be described by effective-mass approximation as

$$\left[-\frac{\hbar^2}{2m^*}\nabla^2 + V(\vec{r})\right]\psi_{\vec{k}}(\vec{r}) = E(k)\psi_{\vec{k}}(\vec{r})$$

[1.1]

Where, m^* is the effective mass; $\hbar$ is the Planck's constant divided 2π; $\vec{r} = (x, y, z)$ is the electron position vector; $V(\vec{r})$ is the confinement potential; $\psi_{\vec{k}}(\vec{r})$ is the wave function (or eigenfunction); and $E(\vec{r})$ is the electron energy(or engenstate). The eigenatates, eigenfunctions and density of state (DOS) for various quantum systems are as follows,

For bulk material,

$$E(\vec{k}) = E(k_x, k_y, k_z) = \frac{\hbar^2}{2m^*}\left(k_x^2 + k_y^2 + k_z^2\right) \quad [1.2]$$

$$\psi_{\vec{k}} = \frac{1}{\sqrt{V}}\exp\left[-i\left(k_x x + k_y y + k_z z\right)\right] \quad [1.3]$$

$$D(E) = \frac{1}{2\pi^2}\left(\frac{2m^*}{\hbar^2}\right)^{3/2} E^{1/2} \quad [1.4]$$

For quantum well,

$$E(\vec{k}) = E_n(k_x, k_y) = \frac{\hbar^2}{2m^*}\left(k_x^2 + k_y^2 + \left(\frac{n\pi}{L_z}\right)^2\right) \quad [1.5]$$

$$\psi_{\vec{k}} = \frac{1}{\sqrt{A}}\varphi_n(z)\exp\left[-i\left(k_x x + k_y y\right)\right] \quad [1.6]$$

Where

$$\varphi_n(z) = \sqrt{\frac{2}{L_z}}\sin\left[n\pi\left(\frac{z}{L_z} + \frac{1}{2}\right)\right] \quad [1.7]$$

$$D(E) = \frac{m^*}{\pi\hbar^2 L_z}\sum_n H(E - E_n) \quad [1.8]$$

For quantum wire,

$$E(\vec{k}) = E_{m,n}(k_x) = \frac{\hbar^2}{2m^*}\left(k_x^2 + \left(\frac{m\pi}{L_y}\right)^2 + \left(\frac{n\pi}{L_z}\right)^2\right) \quad [1.9]$$

$$\psi_{\vec{k}} = \frac{1}{\sqrt{L}}\varphi_m(y)\varphi_n(z)\exp[-ik_x x] \quad [1.10]$$

$$D(E) = \frac{N_{WR}}{\pi}\frac{\sqrt{2m^*}}{\hbar}\sum_{m,n}\frac{1}{\sqrt{E - E_{m,n}}} \quad [1.11]$$

For quantum dot,

$$E(\vec{k}) = E_{l,m,n} = \frac{\hbar^2}{2m^*}\left(\left(\frac{l\pi}{L_x}\right)^2 + \left(\frac{m\pi}{L_y}\right)^2 + \left(\frac{n\pi}{L_z}\right)^2\right) \quad [1.12]$$

$$\psi_{\vec{k}} = \frac{1}{\sqrt{L}}\varphi_l(x)\varphi_m(y)\varphi_n(z) \quad [1.13]$$

$$D(E) = 2N_D\sum_{l,m,n}\delta(E - E_{l,m,n}) \quad [1.14]$$

In Eq. [1.3], $V = L^3$ is the crystal volume. In Eq. [1.6], $A = L^2$ is the area of the quantum well, L_z is the well width, and the $H(x)$ is the Heaviside step function ($H(x) = 1$ for $x \geq 0$ and $H(x) = 0$ for $x < 0$). In Eq. [1.10], L is the length of the quantum wire, L_y is the y-direction length of the wire cross-section, and in Eq. [1.11], N_{WR} is the density of quantum wires. In Eq. [1.14], N_D is the volume density of quantum dots. Fig 1.1 shows the nanostructure and their DOS.

1.2.2 Field Emission Properties

It is well known that nanotubes[40-44] and nanowires[45] with sharp tips are suitable materials for cold cathode field emission device application. Field emission characteristics of these 1D materials have been investigated using current-voltage

measurements and the Fowler-Nordheim (FN) equation recently.[46,47]

The FN current density across an energy barrier ϕ under the effect of an electric field E is described by the FN equation and can be expressed as (Fig. 1.2)

$$J = \frac{1.54\times10^{-6}E^2}{\phi t^2(y)}\exp\left[-6.87\times10^7\frac{\phi^{2/3}v(y)}{E}\right]Acm^{-2} \quad [1.15]$$

where E is the applied electric field of the tip, ϕ is the work function (in eV), $t(y)$ and $v(y)$ are correction factors related to the electric field, and y can be approximated as

$$y = 3.79\times10^{-4}E^{1/2}/\phi \quad [1.16]$$

For simple, the factors $t^2(y)\approx1$ and $v(y) = 0.95 - y^2 \approx 1$. The electric field at the tip can be represented as

$$E = \beta V_g \quad [1.17]$$

where β is the field enhancement factor, and V_g is the voltage applied to the gate and emitter electrodes. Thus, the current of the field emission array is

$$I = nAJ = nA\frac{1.54\times10^{-6}(\beta V_g)^2}{\phi}\exp\left[-6.87\times10^{-7}\frac{\phi^{3/2}v(y)}{\beta V_g}\right] \quad [1.18]$$

where n is the number of emitters and $A(cm^2)$ is the emission area per tip. The logarithmic form of eq. (18) can be expressed as

$$\log\left(\frac{I}{V_g}\right) = \log\left(1.54\times10^{-6}\frac{nA\beta^2}{\phi}\right) - 2.98\times10^7\frac{\phi^{3/2}v(y)}{\beta V_g} \quad [1.19]$$

Consequently, a plot of $\log\left(I/V_g^2\right)$ versus $1/V_g$ yields a straight line with slope m and intercept b giving by following equations:

$$m = -2.84\times10^7\left(\frac{\phi^{3/2}}{\beta}\right) \quad [1.20]$$

$$b = \log\left(1.4\times10^{-6} n\alpha \frac{\beta^2}{\phi} \exp\left(\frac{9.87}{\sqrt{\phi}}\right)\right) \qquad [1.21]$$

1.2.3 Building Blocks for Molecular and Nanotechnology

Current trends in reducing the size of electronics and electromechanical systems have motivated the evolution of new concepts for fabricating electronic nanostructures.[48,49] 1D nanostructures, such as nanowires and nanotubes, are ideal systems for investigating the electrical transport, optical properties and mechanical properties on size and dimension, are building blocks that propose to nano/molecular electronics for future computing.[50] They are expected to play important role as interconnects and functional components in the fabrication of nanoscale electronic and electroptical devices.

Integration of nanowires blocks into complex functional structure is a major challenge in nanowires research. To develop suitable hierarchical assembly techniques to put nanowires building blocks together into functional structure, atomic force microscope has been used to push or deposit nanowires into desired configuration. The disadvantage of this method is it takes a lot of time. The other possibility is use microfluidic assisted nanowires integration process (Fig. 1.3). The microchannels have height 1-4 μm, width of 1-10 μm and lengths of 5-10 mm, are formed between a poly(dimethylsiloxane) (PDMS) micromold and a flat substrate.[51] A drop of solution with nanowires was put at one end of the microchannels, the fluid flow through the channels due to the capillary effect. After the solvent evaporated, these wires were lay along the flow direction limited by the PDMS. By rotating the microchannels during second application, it is possible to assemble the nanowires into functional networks (Fig. 1.4).

Take the Si nanowires as an example, Si nanowires have been demonstrated to function as simple field-effect transistor (FET), and the doped p- and n- type Si nanowires (Fig. 1.5) can be employed to form p-n junction, bipolar transistors, and complementary inverters. The combining of p-type and n-type nanowires through a bottom-up assembly in crossed arrays that could be considered for devices. Theses results propose that the nanowires could be used as components for nanoelectric devices, behaving as both functional units and interconnects.

1.2.4 Probes for Scanning Probe Microscopy (SPM)

The encouraging of smaller and smaller structures and the desire to understanding complex system increases the requirements for imaging and detection tools. Scanning probe microscopy (SPM) represents one of most widely used tools for nanoscale morphology.[53] The resolution of SPM is limited by the size and shape of the probe tip used for imaging. Commercially available probes consist of pyramids of Si or Si_3N_4 that have blunt end. These tips shows constrain on the lateral resolution and likewise, the pyramidal shape impede the ability of these tips to take the narrow and deep features. Recently, a potential to achieve high resolution of SPM technology was by attaching multiwall carbon nanotubes[54, 55] on the end of Si tips. The high aspect ratio nanotubes tips have apparently advantages for probing deep gap and precipitous features and were come to by Dai *at al.*. In addition, the elasticity of nanotubes, reduced the maximum force applied to the sample, which can prevent the organic and biological sample from the damages cause by the tips. Applications of such modified probes provide advantages for high-resolution imaging of nucleic acids and proteins and enable application in biotechnology.

1.3 Overview of the Growth Mechanism of Nanowires

The "top-down" chemical approaches[57] to high quality such as "T-wires" and "V-groove wires"[58] are combine lithography with epitaxial growth technology. "T-wires" have been synthesized by growing semiconductor quantum wells via molecular beam epitaxy (MBE), follow by cleavage and overgrowth on the cleaved surface, while "V-groove nanowires" have been fabricated by etching trenches on the surface and then deposited materials into the grooves. These nanowires synthesized by these methods are embedded in the substrates cannot assemble into complex devices.

Although nanowires can be fabricated using advanced lithography technologies, such as e-beam writing, proximal-probe patterning, and x-ray lithography. However, these methods are slow and high cost, the development of "bottom-up" technologies to rapidly synthesize large numbers of nanowires with low cost represent another important approach to nanowires. An important issue in the study and application of nanowires is how to control the size, dimensionality, interfaces of these nanostructures and assemble them into two-dimensional and three-dimensional functional superstructures.

Since the discovery of carbon nanotubes (CNTs) in 1991, one-dimensional nanowires of elemental and compound semiconductors such as Si,[59-62] Ge,[63,64] InP,[65] GaAs[66] and SnO_2[67] have been synthesized by vapor-liquid-solid （VLS） growth mechanism,[68-70] solution-liquid-solid (SLS) growth mechanism,[71] gas-solid (GS) growth mechanism,[72] laser-assisted catalytic growth (LCG),[73] template-based synthetic approaches,[74] physical vapor deposition (PVD),[75,76] chemical vapor deposition (CVD)[77-80] and oxide-assisted nucleation.[26,81] The ability to synthesized nanometer scale control in diameter during anisotropic crystal growth while

maintaining a good overall crystallinity, large quantities of high pure (contamination-free), ultra long and uniform-sized nanowires from these techniques offer exciting possibilities in fundamental and applied research.

1.3.1 Vapor-Liquid-Solid (VLS) Growth Mechanism

Since the 1964, Si whiskers were synthesized by the well-known VLS growth mechanism (Fig. 1.7). In the VLS growth mechanism, metal particles such as Au, Fe, or Cu, are deposited on the Si substrate used as the mediating solvent.[82-86] The Au forms the Au droplet on the Si substrate. The liquid droplets serve as catalytic sites, which absorb the reactants on the substrate. When droplets supersaturated, the reactants in vapor phase bond to the Si substrate at the liquid-solid interface, and the nanowires grow. The growth directions of these nanowires are decided by the lowest liquid-solid interfacial energy at the liquid-solid interface.

Since the method is originally applied with the liquid metal drops, the minimum of the wires diameter is determined by the diameter of the droplet at the tip.[91] The observation related to the thermodynamic limit for the minimum radius of the alloy droplets at high temperature

$$r_{\min} = \frac{2\sigma_{LV} V_L}{RT \ln s} \qquad [1.22]$$

whereσ_{LV} is the liquid-vapor surface free energy, V_L is the molar volume of liquid, and s is the vapor-phase supersaturation. Therefore, monodisperse nanowires can be synthesized by applying single size metal clusters mediate as catalysts for nanowires growth. Most of the techniques related to the VLS process, the catalyst usually in the nanowires and may affect its intrinsic properties.

1.3.2 Solution-Liquid-Solid (SLS) Growth Mechanism

The SLS growth mechanism[89] (Fig. 1.8) shows that processes analogous to VLS growth can operate at low temperature. The fibers or whiskers prepared by SLS mechanism have diameters of 10 to 150 nanometers and lengths of several micrometers. For example, methanolysis $\{t\text{-}Bu_2In[\mu\text{-}P(SiMe_3)_2]\}_2$ in aromatic solvents gives highly crystalline InP fibers (dimension 10 - 100 nm × 50 - 1000 nm) at temperature as low as 111 - 203 ℃. In this growth mechanism, the reactant dissolve in the solvents resulting $(InP)_n$ fragment absorbed by the molten In droplets and crystallize as the InP nanowires. The defect-free Si nanowires (Fig. 1.9) also synthesized by the SLS growth mechanism. In the process, solvent-dispersed alkanethiol-capped gold nanocrystals catalyze Si nanowires growth at temperature 500℃ and 270 bar.

In the SLS growth mechanism, crystal growth requires (1) a reversible pathway between the fluid (solution, melt or vapor) and the solid phase or (2) high surface mobility in the solid phase. These conditions let the atoms, ions, or molecules to get the correct position developing the crystal lattices. Ionic and molecular solids can be crystallized from solution at low temperature because aqueous or organic solvents dissolve their constituent ions or molecules and condition (1) is met. However, covalent nonmolecular solid such as III-V semiconductors are generally insoluable cannot be crystallized from the solution at low temperature. These materials should be synthesized from solution by condition (2) with two circumstances that support low-temperature crystal growth: catalysis by protic reagents and the participation of metallic flux particles. The low-temperature SLS growth mechanism shown in Fig. 1.8 is analogous to the high-temperature VLS growth mechanism, and the SLS growth mechanism possibly opening the low temperature method to synthesize many

covalent solids such as fibers, whiskers, and quantum dots.

1.3.3 Laser-Assisted Catalytic Growth (LCG)

Compared with the classical VLS growth mechanism,[26] nanoparticles of metal or metal silicide in large quantity are rather easy obtained from the laser ablation method using metal-containing target. The typical experiment was carried out by using excimer laser to ablate the target in an evacuated quartz tube filled with argon gas in which the pressure and temperature are varied (Fig.1.10). The solid target could be high pure powder mixed with metals (Fe, Ni, or Co). The background pressure is used to control condensation and cluster size, while the temperature can be varied to maintain the catalyst cluster in the liquid state.

Nanowires growth initiates after a laser-generated cluster becomes supersaturated and stopped when the nanowires and attached liquid cluster go through the hot zone of the furnace as shown in Fig. 1.10. These variations result in deviation of the mean diameter of the nanowires, and the nanowires produced in this method with broad diameter distribution. In contract to the VLS growth mechanism, those 1D materials grown by the LCG mechanism (Fig. 1.11) often have some structure defects, such as the stacking faults, interface roughness, grain boundary, twins, ect.

1.3.4 Template-Based Synthetic Approaches

Recently, template-based synthesis that used zeolites, membranes, or nanotubes can control growth of nanowires but usually form the polycrystalline materials.[90,91] Template-based synthesis is a convenient method for nanowires growth. These templates have nanoscale channels within mesoporous materials,[92] porous alumina,[93]

carbon nanotubes[94-96] and polycarbonate membranes.[49] This method is used to prepared nanowires,[97] nanotubes[98,99] composed of electronically conductive polymers,[100] metals,[101,102] semiconductors,[93,103] and many other materials.[48,104-106] Besides, these pores in the membranes have monodispersed diameters, analogous monodispersed nanostructure can be obtained.

A number of membranes have been used in this type of template process. Take the anodic alumina membranes (AAM) as an example, a self-assembled nano-porous material formed by anodization of Al in an appropriate acid solution has draw interest as their several unique structure properties such as controllable pore diameter, extremely narrow size distribution for pores diameter and their interval, ideally cylindrical shape of pores. They have been used to fabricated nanosized fibers, nanorods, nanowires, and nanotubes of metals, semiconductors and other solid materials. The AAM occupied hexagonal ordered porous structure with the porous diameters ranging from 10 to 200 nm, porous density in the range 10^{10}-10^{12}/cm^2, and high aspect ratio of the channel, which is difficult to achieve with conventional lithography technology.

After fabricating the AAM template, nanowires can be growth in these nanopores by four methods: (1) Electrochemical deposition of metals, alloys and compounds into the pore of the template; (2) Electrophoretic filling of the pores with colloids; (3) Filling with sol-gel; (4) Filling through CVD or VLS growth mechanism.[107-111] Using AAM, the different kinds of ordered nanowires array have been synthesized. All of these methods are powerful techniques to prepare nanowires of various compositions can provide good control over the length and diameter of nanowires. Expect the VLS growth combines with the template-based method; other methods have the draw back that they often produce polycrystalline materials, which are less suitable for both fundamental and applied studies.

1.4 Research Objectives

1.4.1 Manganese Oxide-Carbon Nanotube Nanocomposite Supercapacitor Electrodes

With the development of technology, energy storage devices, including batteries[112] and supercapacitors[113-118], have drawn much attention for the possibilities of potential applications in power source of various electronic products. The battery is a device that stores electrical energy by an electrochemical reaction, while the supercapacitor stores electrical energy by the physical adsorption and the reversible faradaic redox reaction taking place on the surface of a substrate material. Although the battery exhibits high energy density, the electrochemical stability and power density, it still requires improvement in the reversibility of chemical reaction. Worldwide attention is focus on supercapacitors due to their safety, short charging time, electrochemical stability, high powder density and long cycle life. These supercapacitors can be classified according to the charge storage mechanisms: the electrical double–layer capacitor (EDLC) [114,115] and the faradaic capacitor[116-118]. The EDLC consists of the high specific surface material since the energy storage mechanism is the electronic and ionic charges physically adsorbed on the interface of the double–layer. On the other hand, the faradaic capacitor consists of the several oxidation states material as the mechanism involves not only physical adsorption of electrons and ions, but also the reversible redox reactions occurring on the electrode surface.

The carbon nanotubes (CNTs) are attractive material applied in energy storage devices, such as secondary battery[119], fuel cell[120] and pseudocapacitor[121-123], because of their chemical stability, low mass density, activated high surface area and high

conductivity. The specific capacitances of CNT–based electrodes have been reported to be between 4 and 146.6 F/g in the solution of H_2SO_4, which is relatively lower than that of an activated carbon electrode with large area. To provide enhanced capacitance, composite electrodes, such as activate carbon (AC)–indium tin oxide (ITO)[124], polyaniline–gold nanocluster[125], and RuO_x–VO_2[126] are currently investigated for the supercapacitor applications. Park et al. reported that the RuO_x modification of CNTs provides a composite electrode material that shows a specific capacitance based on the mass of RuO_x and the value is 900F/g.[127] Therefore, the suitably modified transition metal oxides CNTs would form potential composite materials for use in the supercapacitors.

In chapter 3, the manganese oxide–CNTs composite electrode was investigated. The $MnO_x{\cdot}nH_2O$/Ni and $MnO_x{\cdot}nH_2O$/CNTs/Ni electrodes were synthesized by anodic deposition. The crystal structures, surface morphologies and microstructures of these composite electrodes were investigated. The capacitance and rechargeable properties were characterized by cyclic voltammetric method and constant current discharge method. An equivalent circuit model was proposed and demonstrated by an impedance analyzer.

1.4.2 Synthesis of ZnO Nanowires on Polymer Substrate

One-dimensional (1D) nanostructures, such as nanowires (NWs), nanotubes, and nanobelts, have been investigated in the potential applications of photonic, electrooptical and electronic devices for their fascinating physical and chemical properties.[128-131] Due to the high aspect ratio, the 1D nanostructures were studied in vacuum electronic devices, including the cold cathode field emission display (FED), electron sources and high power rf amplifier for their low turn on electric field and

high electron emission efficiency.[130-132]

ZnO with the wide direct band gap (3.4 eV) and large exciton binding energy (60 meV) is of interest for the possible applications in phosphors, transparent conducting films for solar cells, ultra–violet (UV) laser devices, and flat panel displays.[86,133-138] Many previous studies focus on the preparations and electrical properties of the ZnO films.[139-150] Recently, ZnO nanowires (Fig. 1.12), which synthesized by Yang's group[151-153] have been a subject of particular attention; they can be grown in single crystal form, achieve high aspect ratios, exhibit quantum confinement effects at sufficiently small diameters and emit ultraviolet (UV) laser, which can be used in luminescent device applications.[64,154-161] Several methods were employed for synthesizing the ZnO NWs, such as vapor–liquid–solid (VLS) growth,[86] metal–organic vapor phase epitaxy (MOVPE) procedures,[137] template method,[138] hydrothermal method[133] etc.. ZnO NWs–based field emission devices have been reported to perform good emission properties with high stability, low threshold electric field and high current density.[136, 162] At present, one of the most serious problems to fabricate the FED is the high synthesis temperature, which will restrict the selection of substrate materials and integration procedures. Among various fabrication methods, hydrothermal method has the advantages of catalyst-free-growth, low cost, low reaction temperature, large area and uniform production, environmental friendliness and compatibility to the plastic electronics. Therefore, hydrothermal method is proposed to be the suitable fabrication process to synthesize the ZnO NWs for FED.

The flexible field emission devices based on the carbon nanotubes (CNTs) have been developed,[130, 131] however, the field emission property of ZnO NW-based flexible FED is seldom discussed. In chapter 4, the hydrothermal method is adopted to fabricate the ZnO NWs on the polyethylene terephtalate (PET) polymer substrates at a

very low temperature of 75 ^{o}C. The influences of seeding layer on the morphologies of ZnO NWs were carrying out. The optical properties and field emission characteristics of the ZnO NWs with various surface morphologies were also investigated.

1.4.3 Influence of Dopants on Hydrothermal growth ZnO Nanowires

1.4.3.1 Influence of Mg Dopant on ZnO Nanowires

It has been reported that the band–gap tunable $Mg_xZn_{1-x}O$ (MZO) films formed by mixing MgO (ΔE_g = 7.8 eV) with ZnO, and the direct band gap varies from 3.3 to 4.0 eV as the Mg content increases.[163] The crystal structure of MZO is quite similar to the ZnO as the ionic radii of Mg^{2+} (0.57 Å) and Zn^{2+} (0.60 Å) are comparable. With a similarity in crystal structure and modulation in band gap, MZO/ZnO is expected to be a potential quantum well heterostructure in optoelectronic devices.

Although MZO NWs and the MZO/ZnO NW–heterostructures have already been synthesized by MOCVD and MBE[164], these processes are expensive, toxic, and power consuming. In order to overcome all these issues, the hydrothermal method is employed in chapter 5 to provide a low temperature process to fabricate the MZO NWs on the glass substrates. The microstructures, surface morphologies, optical properties and field emission characteristics of the MZO NWs were investigated.

1.4.3.2 Influence of P Dopant on MgZnO Nanowires

It has been reported that the emission characteristics of Si NWs depend on the doping type (*n*- and *p*-type).[165-167] However, the field emission properties of other NWs with various dopants are still unclear. Current trends in developing ZnO-based

optoelectronic devices are focused on synthesizing the reliable *n*-type and *p*-type ZnO.[168,169] But, it was difficult to fabricate reproducible *p*-type ZnO due to self-compensating and low solubility of dopants.[170] Recently, Norton et al. have reported that the $P_{0.02}Mg_{0.1}Zn_{0.9}O$ film performed the stable *p*-type behavior by adding Mg and P together, Mg dopant to increase the band gap and P dopant to introduce the acceptor level.[171,172] In chapter 5, the MZO NWs are fabricated on *p*-type [B-doped, 1–10 Ω cm] Si substrates by hydrothermal method. The P ions were incorporated into part of the MZO NWs to form phosphorus doped MZO NWs (PMZO NWs) by using plasma treatment. The crystal structure, chemical composition, photoluminescence and field emission characteristics of MZO and PMZO NWs on the *p*-type Si (100) substrates were examined. The effect of phosphorus dopant on the properties of MZO NWs was also studied.

1.4.4 Characteristics of Field Emission Triode

Trends in nanotechnology and nanomaterials play an important role in the potential applications of photonic, electrooptical and electronic devices because of their unique physical and chemical properties.[129-131, 173] Especially, it has been a hot topic for the last decades to explore the materials for the flat panel display. The high-aspect-ratio one dimensional (1D) nanostructures have been extensively studied in vacuum microelectronic devices, including the field emission display (FED), electron sources, microwave devices and high power rf-amplifier because of the advantage of low turn-on electric field and high electron emission efficiency.[130-132] The main advantages for the FED are a large area display, high uniformity, high productivity, high brightness, low cost, low power consumption and reliability. From this point of view, triode type FED device with a low driving voltage, high resolution

and controllable electron emission characteristics is the candidate for the new generation of FED devices. There are several field emission devices to effectively control the field emission ability: under-gate[174-176] and planar-gate triodes[177-179].

1.4.4.1 Planar Gated Field Emission Triode

ZnO NW emitters have been reported to perform good emission properties with high stability, low threshold electric field, high emission current density, good emission stability and durability.[136, 162] ZnO NWs have been synthesized by various procedures[137, 177, 180]; however, the main challenge to fabricate the NW-based FED devices is the high synthesizing temperature which retards the integration processes for a FED device structure. The hydrothermal method would offer a superior route for the FED fabrication because of their catalyst-free-growth, low cost, low reaction temperature, large area and uniform production, environmental friendliness and the process compatibility to the VLSI.

Although the field emission triode based on the CNTs and diamond films have been developed,[181, 182] the device based on ZnO NWs is seldom discussed. In chapter 6, the hydrothermal method is adopted to fabricate the ZnO NWs in the field emission triode device at 75 ^{o}C, and the controllable field emission characteristics were investigated.

1.4.4.2 Under Gated Field Emission Triode

Under gate triode with a simple fabrication process, low driving voltage, high resolution under low gate voltage and wide gate bias operation conditions is the candidate for the next generation of FED devices. One of the most serious problems

to integrate the NWs to the FED is the high synthesis temperature, which will restrict the selection of substrate materials and integration procedures. Thus, the hydrothermal method with low synthesis temperature is proposed to be the suitable fabrication process to synthesize the ZnO NWs for FED. The under gate field emission triode based on the carbon nanotubes (CNTs) have been developed[174], however, the field emission property of ZnO NW-based under gate field emission triode hasn't been discussed. In chapter 6, the hydrothermal method is also adopted to integrate the ZnO NWs to the microelectronics at a low temperature of 75 ^{o}C, and the controllable field emission characteristics of the ZnO NWs were investigated.

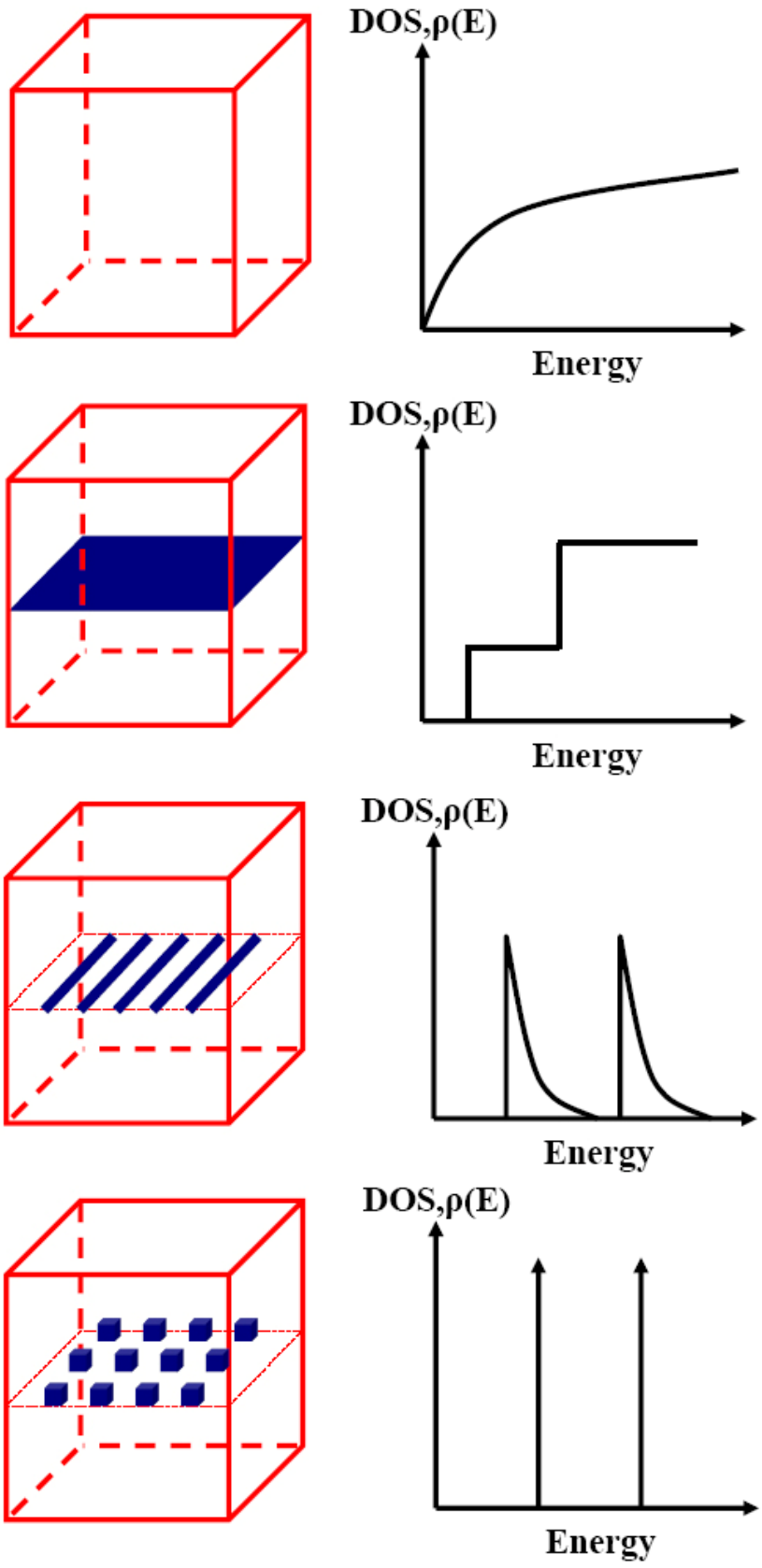

Figure 1.1 The nanostructure and their corresponding density of states.

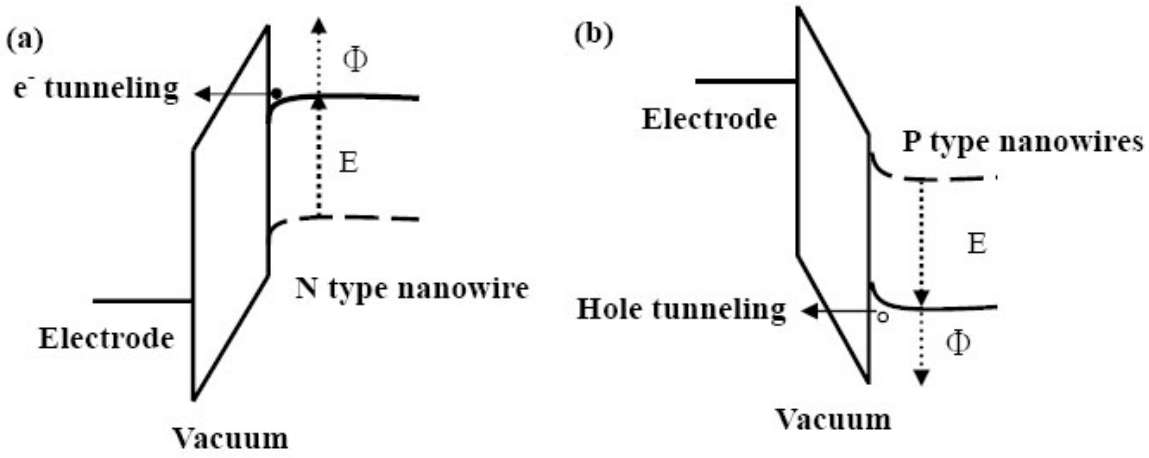

Figure 1.2 Energy band diagram for (a) n type nanowire and (b) p type nanowire in electric fields showing electron and hole tunneling, respectively.

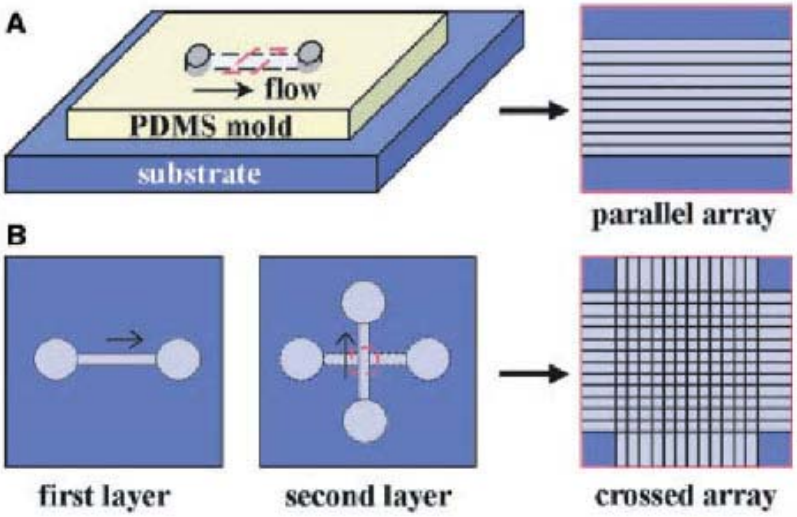

Figure 1.3 The microfluidic assisted nanowires integration process.

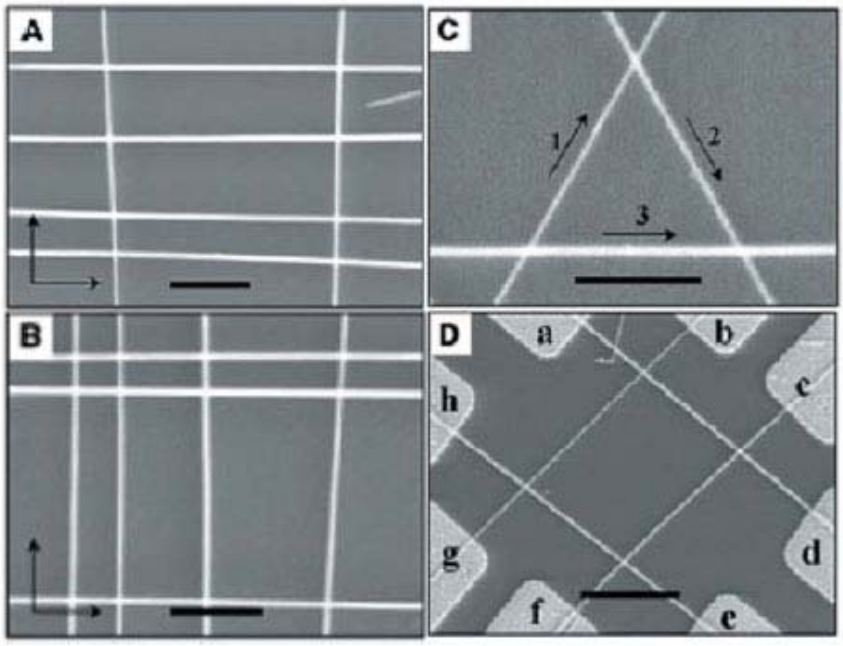

Figure 1.4 Integration of nanowires blocks into complex functional structure by the microfluidic assisted nanowires integration process.

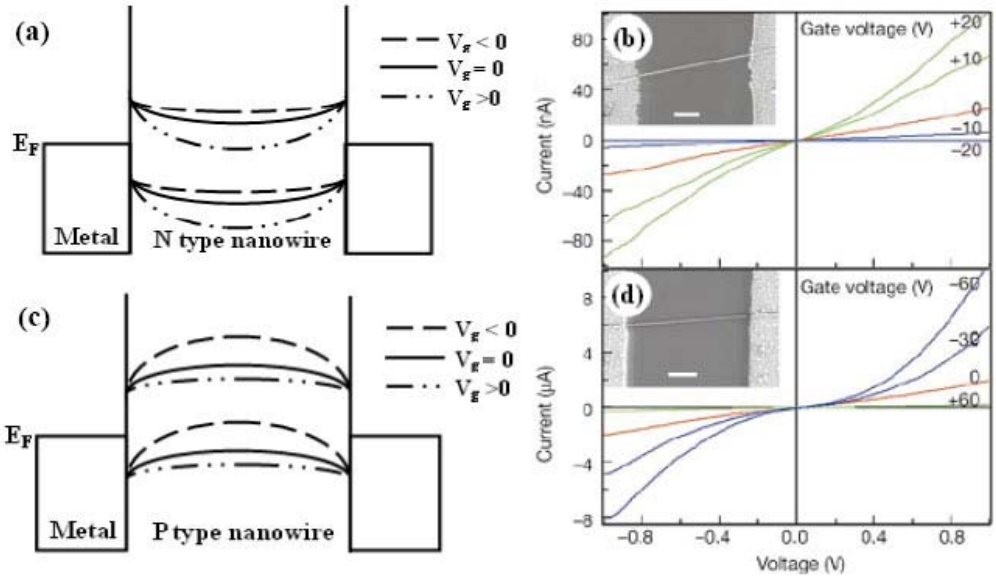

Figure 1.5 (a) The energy band of N type nanowire; (b) Gate-dependent I-V behaviour for N type nanowire; (c) The energy band of P type nanowire; (d) Gate-dependent I-V behaviour for P type nanowire.[52]

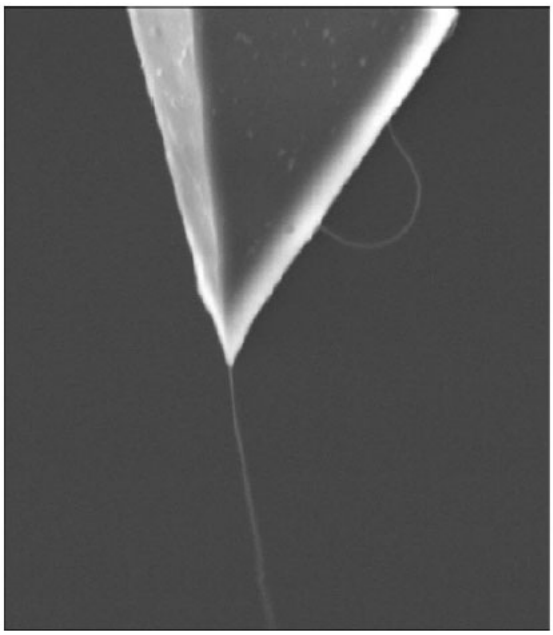

Figure 1.6 The carbon nanotubes probe for SPM.[56]

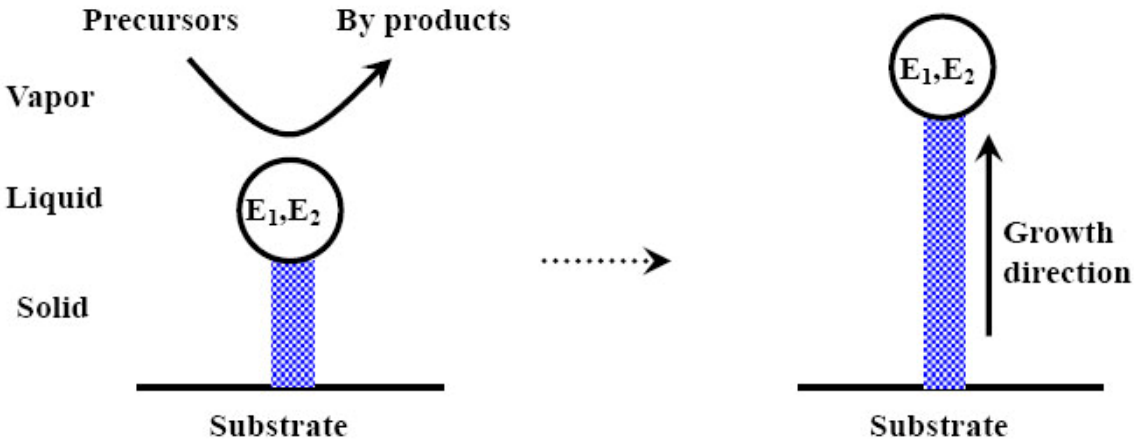

Figure 1.7 The VLS growth mechanism: the droplet is a metal such as Au, Ag, Pd, Pt, Ni, or Cu, and E_1 and E_2 are elements of the crystal phase dissolved in the metallic flux droplet.

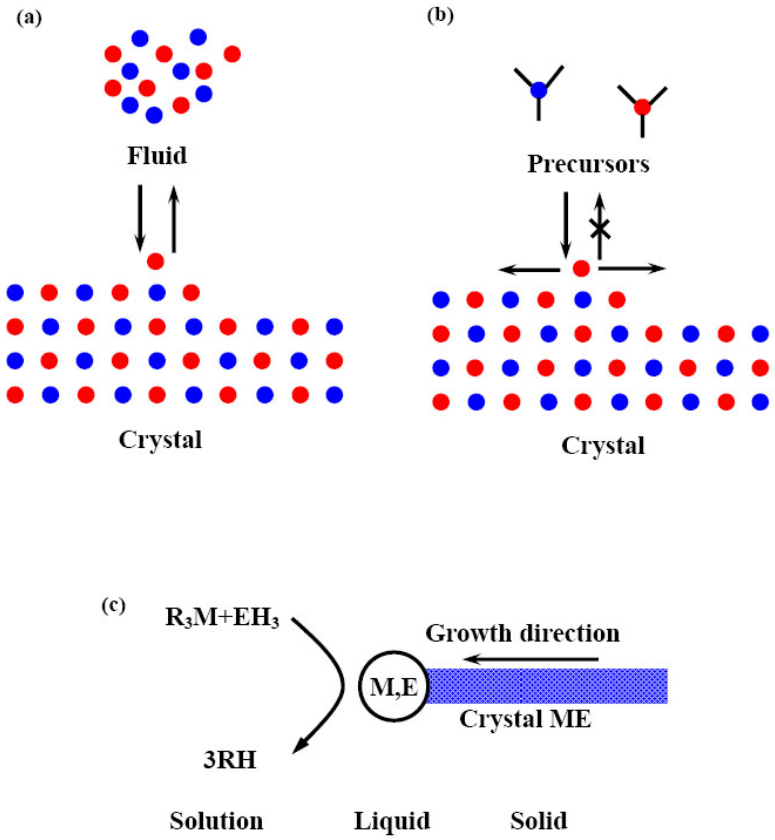

Figure1.8 Crystal growth pathway: (a) growth by reversible deposition from solution, liquid or vapor [condition (1)] (b) growth by irreversible deposition with high solid-phase atomic mobility [condition (2)] (c)SLS mechanism: the flux droplet is In, M and E are elements dissolved in the flux droplet. The crystalline fiber and attached flux droplet are suspended in the solution.

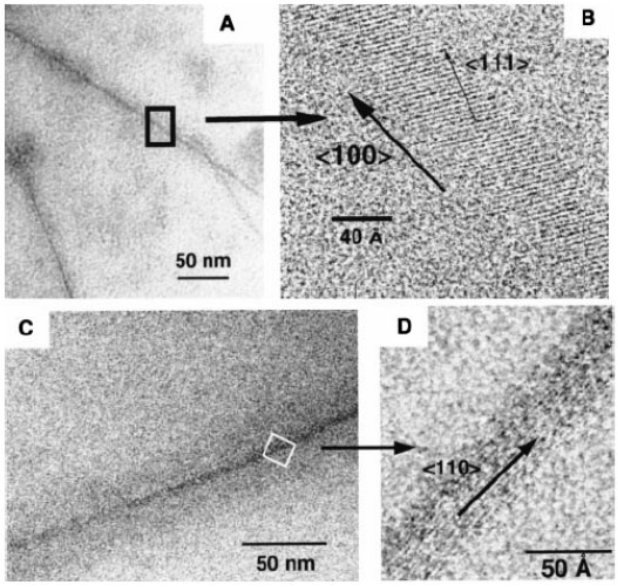

Figure 1.9 The Si nanowires growth by SLS mechanism.

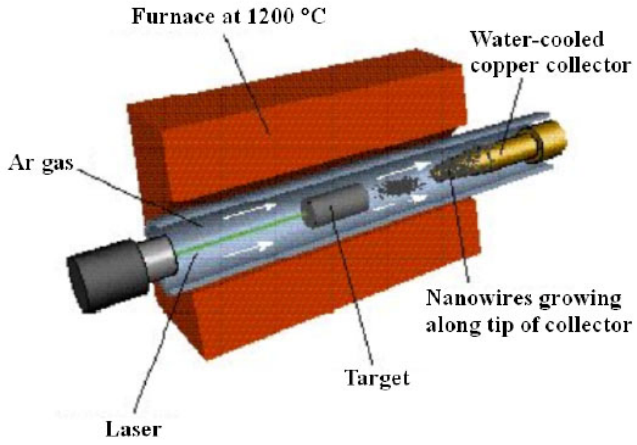

Figure 1.10 Schematic of the LCG growth apparatus.

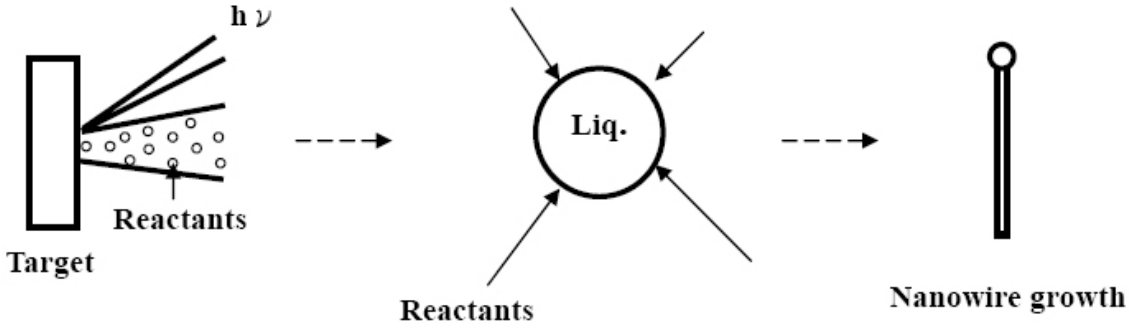

Figure 1.11 The LCG growth mechanism.

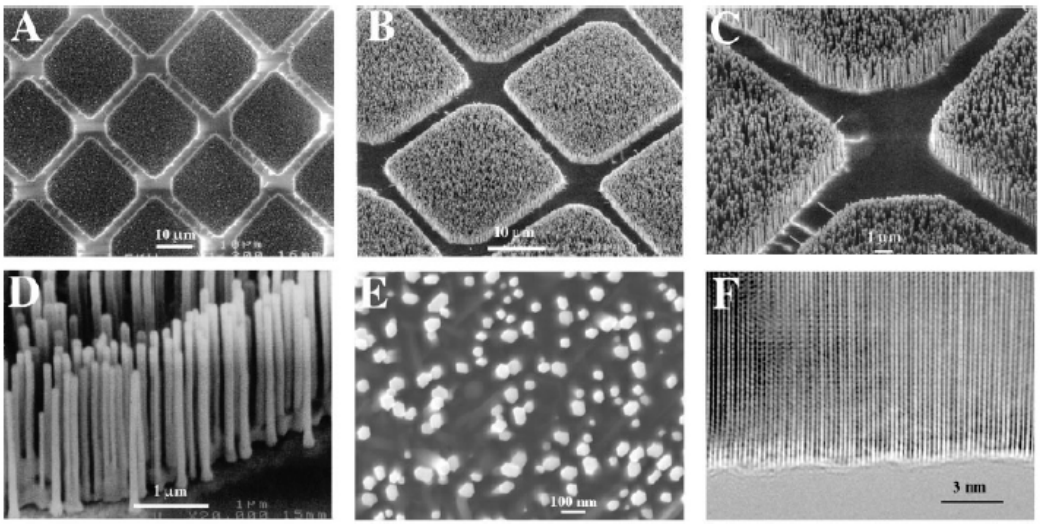

Figure 1.12 The ZnO nanowires fabricated by Yang's group.